Calculations of these solvation energies should be possible when the protein structure becomes available.[50]

As shown in Figure 3A, charge-transfer transitions within the special pair of BChls ($BChl_{LP}$ and $BChl_{MP}$) are expected to have significant effects on the reaction center's spectroscopic properties. We shall analyze these effects further in the following paper[34] and shall show that the theory developed here accounts well for the main features of the absorption, linear dichroism, and circular dichroism spectra of the *Rps. viridis* reaction center. This detailed comparison of the model with experiment is necessary, in order to assess the reliability of the interaction matrix elements. This is critical to an understanding of the initial steps of photosynthesis, because the same type of matrix elements are involved in governing the rate of intermolecular electron transfer.[53,54]

Acknowledgment. This work was supported by National Science Foundation Grants PCM-8303385, PCM-8312371 and PCM-8316161. We also acknowledge with thanks the help of the ISIS program from Digital Equipment Corp. in obtaining the MicroVax II computer on which many of the calculations were done. We thank J. Deisenhofer and H. Michel for providing the crystallographic coordinates, S. Creighton for help with the QCFF/PI calculations, and M. Gouterman, D. Middendorf, R. Pearlstein, and A. Scherz for helpful discussion.

(53) Warshel, A.; Schlosser, D. W. *Proc. Natl. Acad. Sci. U.S.A.* **1981**, *78*, 5564-5568.
(54) Parson, W. W.; Creighton, S.; Warshel, A. In *Primary Processes in Photobiology* Kobayashi, T., Ed.; Springer-Verlag: New York, in press.

Spectroscopic Properties of Photosynthetic Reaction Centers. 2. Application of the Theory to *Rhodopseudomonas viridis*

William W. Parson*† and Arieh Warshel*‡

Contribution from the Department of Biochemistry, University of Washington, Seattle, Washington 98195, and the Department of Chemistry, University of Southern California, Los Angeles, California 90007. *Received November 20, 1986*

Abstract: In the preceding paper [Warshel and Parson, companion paper], a nonphenomenological molecular theory is developed to calculate the spectroscopic properties of the reaction centers of photosynthetic bacteria. We here apply the theory to the reaction center of *Rhodopseudomonas viridis*, whose structure is known from recent X-ray crystallographic studies. Optical absorption, linear dichroism, and circular dichroism spectra are calculated and are compared with the spectra observed experimentally. Intermolecular charge-transfer (CT) transitions between the two bacteriochlorophylls (BChls) of the photochemically reactive special pair ($BChl_{LP}$ and $BChl_{MP}$) appear to make major contributions to the spectroscopic properties. Estimates of the energies of the CT transitions are obtained by exploring how these energies influence the calculated spectra. Good agreement with the observed spectra is obtained by placing the lowest energy CT transition from $BChl_{MP}$ to $BChl_{LP}$ near 14000 cm^{-1}, well above the reaction center's lowest excited state (10400 cm^{-1}), and placing the corresponding CT transition from $BChl_{LP}$ to $BChl_{MP}$ at a substantially higher energy. A large contribution of CT transitions to the reaction center's long-wavelength absorption band is consistent with recent hole-burning experiments and with the sensitivity of this band to external electric fields. Charge-transfer transitions involving the other two BChls ($BChl_{LA}$ and $BChl_{MA}$) are found not to contribute significantly to the spectra. To illustrate the sensitivity of the results to structural features, spectra are calculated as a function of the position of $BChl_{MP}$ and of the orientations of the acetyl groups of $BChl_{LP}$ and $BChl_{MP}$. To model the absorption changes that occur when the special pair of BChls is photooxidized, or when one of the two bacteriopheophytins is reduced, calculations are performed in which one or more of the molecules are omitted from the structure. The absorption changes that occur in the region from 790 to 860 nm reflect a strong mixing of the transitions of all six pigments.

The photosynthetic reaction center of *Rhodopseudomonas viridis* contains four molecules of bacteriochlorophyll *b* (BChl-*b*), two molecules of bacteriopheophytin *b* (BPh-*b*), two quinones, and one atom of non-heme iron, all bound to three polypeptides (L, M, and H). A fourth polypeptide houses four *c*-type hemes. The crystal structure of the reaction center has been solved by X-ray diffraction.[1-3] Two of the four BChls ($BChl_{LP}$ and $BChl_{MP}$) form a closely interacting "special pair" (P) that releases an electron when the reaction center is excited with light. The electron settles on one of the BPhs (BPh_L) with a time constant of about 3 ps[4-6] and then moves to one of the quinones in about 200 ps.[7] The other two BChls ($BChl_{LA}$ and $BChl_{MA}$) sit close by the reactive components,[1-3] but their roles in the electron-transfer reactions are still unclear.

The spectroscopic properties of bacterial reaction centers differ significantly from those of the isolated pigments and have remained poorly understood despite numerous experimental and theoretical studies (see references in the preceding paper[8]). The availability of a crystal structure has now made it possible to explore the spectroscopic properties of the *Rps. viridis* reaction center via detailed theoretical calculations. Such calculations are likely to be most informative if they aim to reproduce the experimental spectra by using calculated molecular parameters or unadjusted experimental parameters obtained with the isolated molecules in solution. This is a more challenging task then the conventional practice of fitting parameters to the observed spectra.

In the preceding paper[8] we developed a theoretical approach capable of predicting the spectra of oligomers of chlorophyll on

† University of Washington.
‡ University of Southern California.

(1) Deisenhofer, J.; Epp, O.; Miki, K.; Huber, R.; Michel, H. *J. Mol. Biol.* **1984**, *180*, 385-398.
(2) Deisenhofer, J.; Epp, O.; Miki, K.; Huber, R.; Michel, H. *Nature (London)* **1985**, *318*, 618-624.
(3) Michel, H.; Epp, O.; Deisenhofer, J. *EMBO J.* **1986**, *5*, 2445-2451.
(4) Woodbury, N. W.; Becker, M.; Middendorf, D.; Parson, W. W. *Biochemistry* **1985**, *24*, 7516-7521.
(5) Martin, J.-L.; Breton, J.; Hoff, A.; Migus, A.; Antonetti, A. *Proc. Natl. Acad. Sci. U.S.A.* **1986**, *83*, 957-961.
(6) Breton, J.; Martin, J.-L.; Migus, A.; Antonetti, A.; Orszag, A. *Proc. Natl. Acad. Sci. U.S.A.* **1986**, *83*, 5121-5125.
(7) Holten, D.; Windsor, M. W.; Parson, W. W.; Thornber, J. P. *Biochim. Biophys. Acta* **1978**, *501*, 112-126.
(8) Warshel, A.; Parson, W. W. *J. Am. Chem. Soc.*, preceding paper in this issue.

0002-7863/87/1509-6152$01.50/0

the self-consistent-field/configuration-interaction (SCF/CI) level. The theory includes intermolecular charge-transer (CT) transitions explicitly and treates exciton interactions with use of transition monopoles rather than point-dipole approximations. The present paper applies our approach to the reaction center of *Rps. viridis*. The calculations succeed in reproducing the main features of the experimental absorption, circular dichroism, and linear dichroism spectra and allow us to address the correlation between the structure and the electronic states of the reaction center. Some of the results have been presented in a preliminary communication.[9]

Methods

Atomic coordinates for the BChl and BPh molecules in the *Rps. viridis* reaction center were kindly provided by Drs. J. Deisenhofer and H. Michel. These coordinates are based on X-ray diffraction data to 3.0-Å resolution.[1-3] Adjustments in the coordinates are to be anticipated as data to higher resolution are included and as information on the amino acid sequence is taken into account.

The energies, dipole strengths, and rotational strengths of the reaction center's absorption bands were calculated as described in the accompanying paper.[8] The Q_y, Q_x, B_x, and B_y transitions of the monomeric BChls were assigned energies of 12 050, 16 670, 24 390, and 27 030 cm^{-1}, respectively, corresponding to wavelengths of 830, 600, 410, and 370 nm. The transitions of BPh_L were put at 12 420, 18 350, 25 000, and 27 380 cm^{-1} (805, 545, 400, and 365 nm), and those of BPh_M were put at 12 580, 18 690, 25 000, and 27 380 cm^{-1} (795, 535, 400, and 365 nm). These wavelengths are close to those found for monomeric BHl-*b* and BPh-*b* in solution. The BChl Q_y transitions, which occur at about 790 nm in solution,[9] were moved to a somewhat longer wavelength to allow for the effects of interactions with the protein (see below). Note that all four BChls were treated identically in this regard. The reason for assigning slightly different energies to the transitions of the two BPhs is discussed below.

To illustrate the calculated absorption spectrum, the contribution from each absorption band was expressed as a molar extinction coefficient (ϵ_i) with an asymmetric Gaussian frequency dependence. For each Gaussian, the maximum extinction coefficient is

$$\epsilon_{i,max} = 1.02 \times 10^2[(n^2 + 2)^2/9n]|\mu^T_i|^2\Delta E^T_i/W_i \ M^{-1}\ cm^{-1} \quad (1)$$

where n is the refractive index, $|\mu^T_i|^2$ is the dipole strength (in D^2), ΔE^T_i is the excitation energy (in cm^{-1}), and W_i is the full width of the band (in cm^{-1}) at half-maximal amplitude. For the CD spectrum, the difference between the maximal extinction coefficients for left- and right-handed circularly polarized light is

$$\epsilon_{l,i,max} - \epsilon_{r,i,max} = 3.79 \times 10^{-6}[(n^2 + 2)^2/9n]\mathcal{R}^T_i\Delta E^T_i/W_i \ M^{-1}\ cm^{-1} \quad (2)$$

where $\mathcal{R}^T_i$ is the rotational strength in $D\cdot\mu_B$. The refractive index was taken to be that of water (1.33).

The following widths were assigned to the 32 bands that were included in the calculations for Figure 3: 500 cm^{-1} for bands 2 and 3; 1000 cm^{-1} for 1 and 4–6; 1200 cm^{-1} for 10, 11, 14, and 15; 1500 cm^{-1} for 8 and 9; 2000 cm^{-1} for 7, 12, 13, and 16; 2500 cm^{-1} for 17–22; 2800 cm^{-1} for 23–28; and 3000 cm^{-1} for 29–32. The bands are numbered in order of increasing energy (ΔE^T_i, see Table I.) To simulate the intrinsic asymmetry of the absorption bands of BChl and BPh[10,11] the half-width of each Gaussian was increased by 10% of the full width on the high-energy side of the maximum and decreased by the same amount on the low-energy side. Because overlapping bands with opposite signs tend to cancel, the calculated CD and linear dichroism spectra are sensitive to the choices of the bandwidths. The widths used here are similar to those of BChl-*b* and BPh-*b* in solution but are increased somewhat for bands that are largely charge transfer in character. We did not attempt to optimize the widths systematically. When BPh_L or the special pair of BChls were omitted from the calculations (Figure 6), the widths assigned to the bands that remained in the spectrum were the same as those of the bands with corresponding excitation energies in the full set.

Linear dichroism (Table I and Figure 3B) was calculated with the expression

$$|\mu^T_i|^2_\perp - |\mu^T_i|^2_\parallel = (3/2)(1 - 3\cos^2\theta_i)|\mu^T_i|^2 \quad (3)$$

for each of the absorption bands, where θ_i is the angle between the band's overall transition dipole (μ^T_i) and the reaction center's local axis of rotational pseudosymmetry. This corresponds to the linear dichroism of a sample with perfect uniaxial orientation with respect to the symmetry axis.[12] Transitions that are polarized perpendicular to the symmetry axis are considered to have positive linear dichroism, to conform with the convention used by Breton.[12]

In the calculations in which the acetyl group of $BChl_{LP}$ was rotated (Figure 5C), we included the changes in the electric and magnetic transtion dipoles and energies of the local transitions (Q_y, Q_x, B_x, and B_y) of this BChl. The change in the transition energy is given by

$$\Delta(\Delta E_k) = \Delta\{-\textstyle\sum_N(c_{k,N})^2(v_{n2,s}v_{n2,t} - v_{n1,s}v_{n1,t})(1.94 \times 10^4\ cm^{-1})\cos\varphi_{s,t}\} \quad (4)$$

where $v_{n1,s}$ and $v_{n1,t}$ are the atomic expansion coefficients for molecular orbital ϕ_{n1} on atoms s and t (s and t = carbons 3 and 20 of $BChl_{LP}$ with the atoms numbered in Figure 1A of ref 8), $v_{n2,s}$ and $v_{n2,t}$ are the corresponding coefficients for orbital ϕ_{n2}, $c_{k,N}$ is the configuration interaction (CI) coefficient for the excitation from ϕ_{n1} to ϕ_{n2} in transition k (k = Q_y, Q_x, B_x, B_y) and $\varphi_{s,t}$ is the torsional angle of the C3–C20 bond. The angle is defined to be zero when atom O1 lies in the plane of atoms C4, C3, and C20 (see Figure 1 of ref 8). The calculations illustrated in parts A, B, and C of Figure 5 also included the effects of the displacement or rotation on the energies of the CT transitions, which were found by using eq 5a of ref 8 with the atomic Coulomb integrals reduced by an effective dielectric constant of 3, as well as the effects on all of the off-diagonal terms of the interaction matrix **U**. As a simplifying approximation for Figure 5C, we used a fixed set of molecular orbital and CI coefficients calculated with $\varphi_{s,t} = 0$ (Tables I and II in ref 8), rather than recalculating the coefficients as $\varphi_{s,t}$ was varied.

The electrochromic effects of P^+ on the optical transitions of the other pigments (Figure 6) were calculated with the expression

$$\Delta(\Delta E^b_k) = -\textstyle\sum_a f_a\sum_N(c_{k,N})^2\sum_{s,t}(v_{2,s})^2[(v_{n2,t})^2 - (v_{n1,t})^2]\gamma_{s,t}/D \quad (5)$$

Here $\Delta(\Delta E^b_k)$ is the change in the energy of local transition k of molecule b ($BChl_{LA}$, $BChl_{MA}$, BPh_L, or BPh_M); f_a is the fraction of the positive charge of P^+ that resides on BChl a ($BChl_{LP}$ or $BChl_{MP}$); $v_{2,s}$ is the expansion coefficient for molecular orbital ϕ_2 on atom s of BChl a; $v_{n1,t}$ and $v_{n2,t}$ are the coefficients for orbitals ϕ_{n1} and ϕ_{n2} on atom t of molecule b; $\gamma_{s,t}$ is the semiempricial atomic Coulomb integral (see ref 8); and D is the effective dielectric constant. For simplicity, we assumed that $f_{LP} = f_{MP} = {}^1/_2$ and set $D = 3$, the same value of D that was used for Figure 5. The changes in the local transition energies were added to the diagonal terms of **U** (ΔE_k) before the interaction matrix was diagonalized. A similar expression was used for the electrochromic effects of BPh_L^- on the local transitions of the four BChls and BPh_M

$$\Delta(\Delta E^b_k) = \textstyle\sum_N(c_{k,N})^2\sum_{s,t}(v_{3,s})^2[(v_{n2,t})^2 - (v_{n1,t})^2]\ \gamma_{s,t}/D \quad (6)$$

where $v_{3,s}$ is the expansion coefficient for ϕ_3 on atom s of BPh_L. For a CT transition, the sum over t in eq 6 includes the atoms of both of the BChls that participate in the transition. ($v_{n1,t}$ is

(9) Parson, W. W.; Scherz, A.; Warshel, A. In *Antennas and Reaction Centers of Photosynthetic bacteria*; Michel-Beyerle, M. E., Ed.; Springer-Verlag: Berlin, 1985; pp 122–130.
(10) Scherz, A.; Parson, W. W. *Biochim. Biophys. Acta* **1985**, *766*, 666–678.
(11) Knapp, E. W.; Scherer, P. O. J.; Fischer, S. F. *Biochim. Biophys. Acta* **1986**, *852*, 295–305.
(12) Breton, J. *Biochim. Biophys. Acta* **1985**, *810*, 235–245.

nonzero only for atoms of the donor molecule; $v_{n2,t}$, only for the acceptor.)

Results and Discussion

Charge-Transfer Transition Energies. Our basic strategy is to use the wave functions of isolated, monomeric BChl and BPh molecules[8] as *unadjusted* parameters for calculating the properties of the reaction center. Unfortunately, without sufficiently detailed information on the structure of the protein, one faces uncertainties with regard to the effects of the protein on the zero-order transition energies of the monomers and on the energies of the intermolecular CT states. Probably the largest uncertainties are associated with the energies of the CT states. One can, however, position the key CT energies within a reasonably small range on the basis of potentiometric data and theoretical considerations. The behavior of the calculated spectrum then can be explored as the CT energies are varied within this range.

A *lower limit* for the free energy change associated with the lowest CT transition can be obtained by subtracting the electrochemical potentials for reduction of BChl to the anionic π-radical ($BChl^-$) and for reduction of the cationic π-radical ($BChl^+$), as measured in organic solvents containing small electrolytes. With BChl-*a*, the difference between the two potentials is 1.5 V.[13] This implies that the electron-transfer reaction to form the radicals at infinite separation in a polar solution involves a free energy increase of 1.50 eV or 12 200 cm^{-1}.[15] The free energy change probably is similar in the case of BChl-*b* (ref 14 and J. Fajer, personal communication). The energy of the CT state at a given separation of the unbound radicals in a polar solvent can be estimated from the expression[15-17]

$$\Delta G^{w}_{ct} \approx \Delta G^{w}_{ct,\infty} - (119\ cm^{-1})\sum_{t,s} q^{a}_{t} q^{b}_{s}/Dr_{t,s} \qquad (7)$$

where q^{a}_{t} and q^{b}_{s} are the residual charges on atom t of radical a and on atom s of radical b, D is the dielectric constant, $r_{t,s}$ is the distance between atoms t and s (in Å), and $\Delta G^{w}_{ct,\infty}$ is the energy at infinite separation.

The term $(119\ cm^{-1})\sum_{t,s} q^{a}_{t} q^{b}_{s}/Dr_{t,s}$ in eq 7 is generally small (<20 cm^{-1}) in a solvent of high dielectric constant, even at 3-Å separation,[15-17] so $\Delta G^{w}_{ct} \approx \Delta G^{w}_{ct,\infty} \approx 12\,200\ cm^{-1}$. At issue, however, is the energy of the CT state when the donor and acceptor are in their binding sites on the protein. When the BChl molecules are bound to the protein, the free energy change associated with the CT transition is given by

$$\Delta G^{p}_{ct} \approx \Delta G^{w}_{ct} + (\Delta G^{p}_{sol} - \Delta G^{w}_{sol}) \qquad (8)$$

where ΔG^{p}_{sol} and ΔG^{w}_{sol} are the energies of "solvation" of the radicals by the protein and by the solution, respectively.[15-17] ΔG^{p}_{sol} and ΔG^{w}_{sol} are both relative to the energies of solvation of the neutral species by the protein and the solution. In a polar solvent, the solvation energy ΔG^{w}_{sol} can be quite large. Microscopic calculations of the type described in ref 18 give about 7000 cm^{-1} for the solvation of the pure CT state of a BChl dimer in water. The stabilization of ionic configurations by proteins can be even somewhat greater than that by water.[15] In the reaction center, however, the $BChl^+BChl^-$ CT state must be created by excitation of the uncharged molecules, and it has a lifetime of, at most, only a few ps. The protein probably provides only a relatively small reorganization energy for the initial charge separation process[18,19] and is not likely to relax fully around the dimer on this time scale. This point is supported by recent hole-burning experiments, which indicate that the reorganization energy for the initial relaxation of the excited state is on the order of 200 cm^{-1}.[20-24] The stabilization of the CT state by the protein dipoles thus appears to be much smaller than that of a fully solvated radical-pair in solution. It is important to note in this regard that the actual excimer state in the reaction center involves only a partial contribution of the pure CT state (see below). The polarization of the surrounding solvent by the mixed state will give a smaller solvation energy to the CT state than the energy that would be obtained from a fully polarized solvent. Thus we conclude that $\Delta G^{p}_{ct} > \Delta G^{w}_{ct,\infty} \approx 12\,200\ cm^{-1}$. This means that the lowest CT transition lies above the lowest local (Q_y) transition, which is near 12 200 cm^{-1} for BChl-*b* in solution.

An approximate *upper* limit for the CT energy in the protein can be obtained from SCF molecular orbital calculations that consider the molecules in a vacuum. For the geometry of the special pair of BChls in the *Rps. viridis* reaction center, the lowest CT transition is calculated to have an energy of approximately 16 400 cm^{-1}.[8] Previous calculations for other chlorophylls[25,26] and recent ab initio calculations for porphyrins[27] have given similar results. In principle, calculations for the dimer in a vacuum give an upper limit of the energy and overemphasize the dependence of the energy on the distance between the two radicals, because they do not consider the solvation energy, ΔG^{p}_{sol} (eq 6). However, such calculations also are sensitive to uncertainty in the molecular orbital energies. If the orbital energies are scaled to agree with the experimental Q_y transition energy for monomeric BChl, the estimate of the CT energy is decreased to approximately 13 400 cm^{-1}.[8]

To explore how the energies of CT transitions between $BChl_{LP}$ and $BChl_{MP}$ could affect the spectroscopic properties of the reaction center, we varied the energies over what appeared to be plausible ranges and calculated the dipole strength, rotational strength, and linear dichrosim associated with each of the 32 excited states obtained by diagonalizing the interaction matrix **U**. Figure 1 shows some of the results of calculations in which the four CT energies for electron transfer from $BChl_{LP}$ to $BChl_{MP}$ were assumed to be the same as the energies of the corresponding transitions in the opposite direction, from $BChl_{MP}$ to $BChl_{LP}$. Figure 2 presents calculations in which the former energies were assumed to be higher than the latter by 4000 cm^{-1}. The abscissa in each figure gives the energy of the lowest energy CT transition (from ϕ_2 of one BChl to ϕ_3 of the other); the three higher transitions in the same direction were assumed to lie above this one by 8000, 13 000, and 21 000 cm^{-1}.[8] In both Figures 1 and 2, panel A shows the calculated wavelengths of the absorption bands in the region from 575 to 1100 nm; panels B and C show the dipole strengths and rotational strengths of some of the bands in the near-infrared region.

As the energy of the CT basis state is decreased over the range covered in Figures 1 and 2, the lowest energy absorption band moves to progressively longer wavelengths and loses dipole strength. These trends reflect an increasing contribution of the lowest CT transition in the excited state. Wavelengths and dipole strengths that are consistent with the observed spectroscopic properties of the reaction center's long-wavelength absorption band (approximately 960 nm and 100 D^2) can be obtained by setting the lowest energy CT transition near 15 000 cm^{-1} if the energies for electron transfer in either direction are assumed to be identical (Figure 1) or near 14 000 cm^{-1} if electron transfer from $BChl_{MP}$

(13) Fajer, J.; Brune, D. C.; Davis, M. S.; Forman, A.; Spaulding, L. D. *Proc. Natl. Acad. Sci. U.S.A.* **1975**, *72*, 4956–4960.
(14) Davis, M. S.; Forman, A.; Hanson, L. K.; Thornber, J. P.; Fajer, J. *J. Phys. Chem.* **1975**, *83*, 3325–3332.
(15) Warshel, A.; Schlosser, D. W. *Proc. Natl. Acad. Sci. U.S.A.* **1981**, *78*, 5564–5568.
(16) Warshel, A. *Isr. J. Chem.* **1981**, *218* 341–347.
(17) Warshel, A.; Russell, S. T. *Q. Rev. Biophys.* **1948**, *17*, 283–422.
(18) Churg, A. K.; Weiss, R. M.; Warshel, A.; Takano, T. *J. Phys. Chem.* **1983**, *87*, 1683–1694.
(19) Warshel, A. In *Electron Transport and Oxygen Utilization*; Ho, C., Ed.; Elsevier: Amsterdam, 1982; pp 112–115.
(20) Meech, S. R.; Hoff, A. J.; Wiersma, D. A. *Chem. Phys. Lett.* **1985**, *121*, 287–292.
(21) Boxer, S. G.; Lockhart, D. J.; Middendorf, T. R. *Chem. Phys. Lett.* **1986**, *123*, 476–482.
(22) Boxer, S. G.; Middendorf, T. R.; Lockhart, D. J. *FEBS Lett.* **1986**, *200*, 237–241.
(23) Meech, S. R.; Hoff, A. J.; Wiersma, D. A. *Proc. Natl. Acad. Sci. U.S.A.* **1986**, *83*, 9464–9468.
(24) Hayes, J. M.; Small, G. J. *J. Phys. Chem.* **1986**, *90*, 4928–4931.
(25) Warshel, A. *J. Am. Chem. Soc.* **1979**, *101*, 744–746.
(26) Warshel, A. *Proc. Natl. Acad. Sci. U.S.A.* **1980**, *77*, 3105–3109.
(27) Petke, J. D.; Maggiora, G. M. *J. Chem. Phys.* **1986**, *84*, 1640–1652.

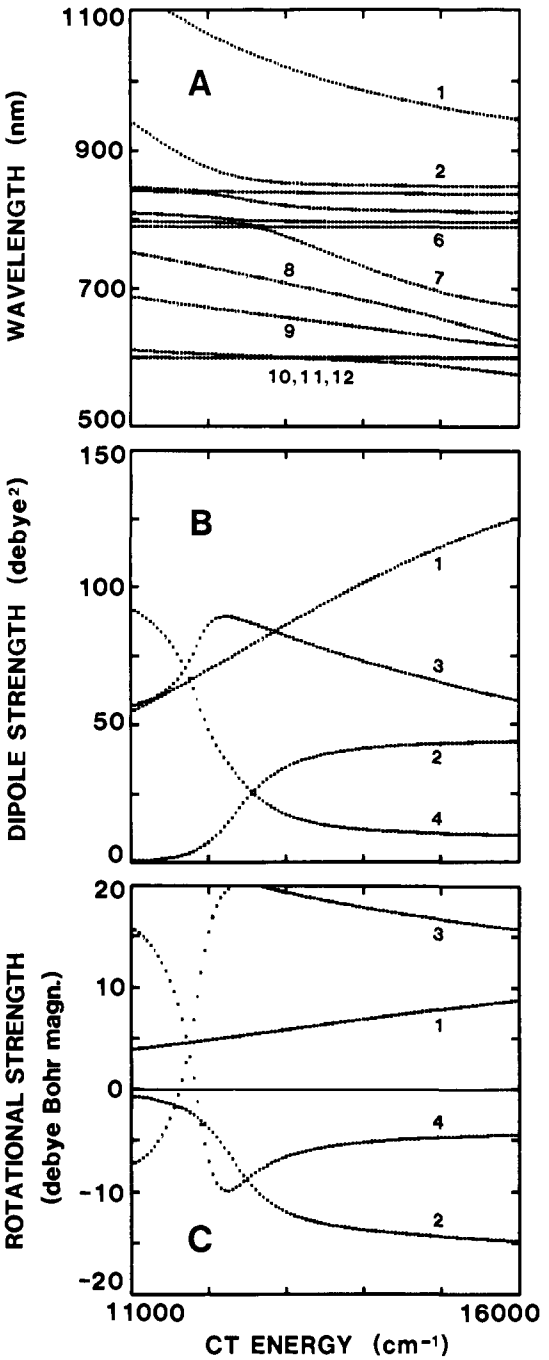

Figure 1. Calculated wavelengths of the *Rps. viridis* reaction center's first 12 absorption bands (A) and the dipole strengths (B) and rotational strengths (C) of the first 4 bands, as functions of the assumed energies of the CT transitions from $BChl_{MP}$ to $BChl_{LP}$. The abscissa gives the energy of the lowest CT transition; the three higher energy CT transitions from $BChl_{MP}$ to $BChl_{LP}$ were placed above this one by 8000, 13000, and 21000 cm^{-1}. The CT transitions from $BChl_{LP}$ to $BChl_{MP}$ were assumed to have the same energies as the corresponding transitions from $BChl_{MP}$ to $BChl_{LP}$. CT transitions involving $BChl_{LA}$ and $BChl_{MA}$ were neglected. The excitation energies assigned to the local transitions of the 6 pigments are given in the text (Methods). The absorption bands are numbered in order of increasing energy.

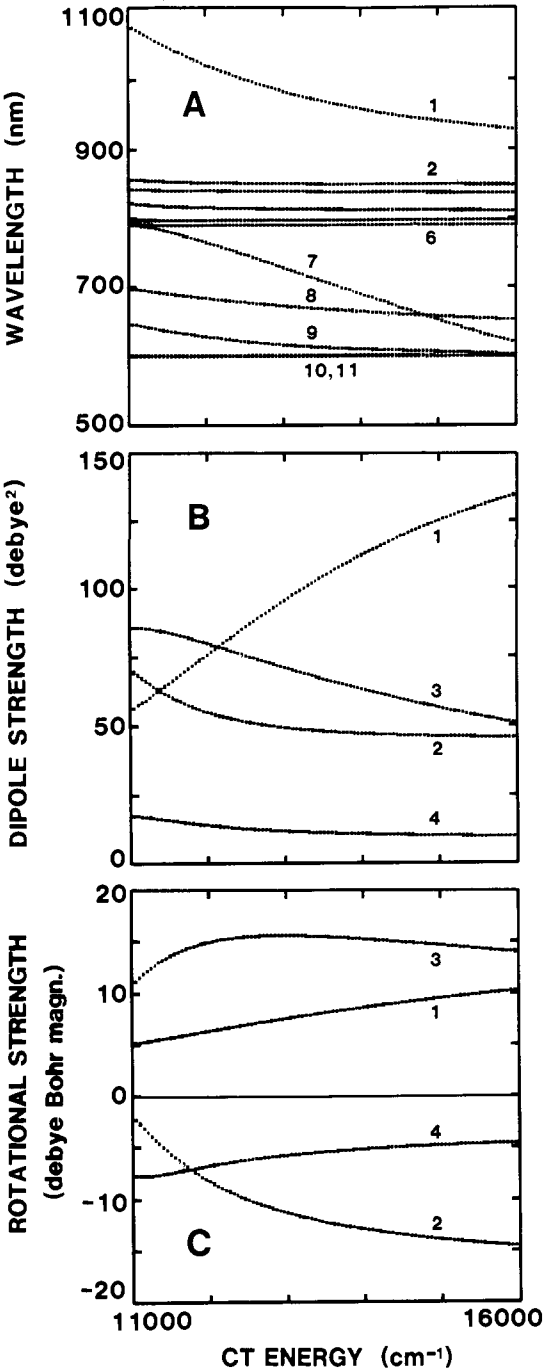

Figure 2. Wavelengths of the first 11 absorption bands (A) and dipole strengths (B) and rotational strengths (C) of the first 4 bands, calculated with the same assumptions as in Figure 1 except that the CT transitions from $BChl_{LP}$ to $BChl_{MP}$ were assumed to lie 4000 cm^{-1} above the corresponding transitions from $BChl_{MP}$ to $BChl_{LP}$.

to $BChl_{LP}$ is assumed to be 4000 cm^{-1} more favorable than that in the opposite direction (Figure 2). In either case, the lowest CT transition must be placed significantly above the local Q_y transitions (12200 cm^{-1}) and the reaction center's lowest excited state (10400 cm^{-1}). This conclusion agrees with our minimal estimate of the free energy increase associated with the CT transition.

In both Figures 1 and 2, note that the dipole strength of the long-wavelength transition can exceed the sum of the Q_y dipole strengths of two monomeric BChls (approximately 100 D^2). This reflects exciton interactions with the other BChls and BPhs of the reaction center, along with hyperchromism that results from mixing of the Q_y and B_y transitions.[10] The composition of the lowest excited state will be discussed in more detail in the following section.

Compositions of the Reaction Center's Excited States. Table I lists the coefficients $C_{i,j}$ that describe the contributions of the 32 basis transitions to the reaction center's first 12 excited states when the energies for electron transfer from $BChl_{MP}$ to $BChl_{LP}$ are put 2000 cm^{-1} below those for transfer in the opposite direction, and the lowest CT transition is assigned an energy of 14400 cm^{-1}. The coefficients do not reflect contributions to the absorption bands stemming from the mixing of doubly excited states in the ground state, but these do not modify the nature of the absorption bands

Table I. Calculated Properties of the First 12 Absorption Bands of the *Rps. viridis* Reaction Center and Coefficients of the 32 Principal Transitions that Contribute to These Bands

		1	2	3	4	5	6
wavelength[a]		958.8	849.3	837.8	812.5	797.8	790.4
dipole str.[b]		114.7	45.0	63.4	10.7	21.1	28.1
rot. str.[c]		8.4	−13.6	15.9	−5.0	1.7	−2.4
lin. dichr.[d]		171.5	−127.3	94.8	−26.3	−13.4	−40.8
perm. dipole[e]		2.8	0.6	0.1	0.2	1.1	1.3
				Coefficients			
BChl (LP)	Q_y	−0.6495	−0.4138	0.0470	0.4715	0.1011	0.0559
	Q_x	0.0093	0.0272	0.0132	−0.0347	−0.0032	−0.0024
	B_x	0.0051	−0.0031	−0.0095	0.0075	−0.0031	−0.0005
	B_y	−0.0349	−0.0008	−0.0100	−0.0171	−0.0043	−0.0039
BChl (MP)	Q_y	0.5705	−0.4455	−0.1641	0.5740	0.1389	0.0660
	Q_x	−0.0525	0.0004	0.0129	0.0031	0.0008	0.0046
	B_x	−0.0192	−0.0100	0.0042	0.0111	0.0020	−0.0021
	B_y	0.0374	−0.0012	0.0092	−0.0246	−0.0091	−0.0043
BChl (LA)	Q_y	0.1266	−0.6058	0.5334	−0.3130	−0.4802	−0.0470
	Q_x	0.0138	−0.0019	0.0031	−0.0040	0.0122	0.0002
	B_x	−0.0297	−0.0120	−0.0039	0.0202	−0.0081	0.0018
	B_y	0.0178	−0.0145	0.0049	0.0079	0.0211	0.0026
BChl (MA)	Q_y	−0.1152	−0.4185	−0.7335	−0.3806	−0.0353	−0.3546
	Q_x	−0.0121	0.0004	−0.0017	−0.0011	−0.0008	0.0080
	B_x	0.0253	−0.0137	−0.0012	0.0171	0.0045	−0.0063
	B_y	−0.0160	−0.0105	−0.0070	0.0100	0.0018	0.0191
BPh (L)	Q_y	0.0464	−0.2452	0.2655	−0.3683	0.8540	0.0343
	Q_x	0.0008	0.0046	−0.0050	0.0072	0.0059	0.0010
	B_x	−0.0002	0.0086	−0.0083	0.0114	0.0094	0.0013
	B_y	−0.0060	0.0113	−0.0093	0.0028	0.0071	0.0006
BPh (M)	Q_y	−0.0364	−0.1228	−0.2546	−0.2197	−0.0859	0.9287
	Q_x	−0.0023	0.0008	0.0022	0.0041	0.0008	0.0016
	B_x	−0.0028	0.0041	0.0078	0.0096	0.0015	0.0047
	B_y	0.0051	0.0066	0.0111	0.0037	0.0002	0.0047
CT (L → M)[f]	1	0.2449	−0.0468	−0.0601	0.0788	0.0226	0.0079
	2	0.0011	−0.0061	−0.0018	0.0090	0.0018	0.0019
	3	−0.0315	−0.0202	0.0031	0.0243	0.0054	0.0030
	4	−0.0228	0.0125	0.0081	−0.0190	−0.0049	−0.0023
CT (M → L)[f]	1	−0.3811	−0.0753	0.0900	0.0799	0.0127	0.0121
	2	0.0491	0.0510	0.0018	−0.0648	−0.0134	−0.0080
	3	0.0432	0.0067	−0.0112	−0.0070	−0.0012	−0.0012
	4	0.0226	0.0067	−0.0048	−0.0075	−0.0013	−0.0010
		7	8	9	10	11	12
wavelength[a]		680.8	669.0	617.8	600.1	599.9	572.6
dipole str.[b]		10.2	0.3	10.8	2.1	12.9	8.0
rot. str.[c]		−0.5	−2.6	3.9	1.9	−2.6	−3.4
lin. dichr.[d]		14.4	0.5	−13.7	−0.7	18.3	6.1
perm. dipole[e]		13.3	6.1	5.9	1.5	1.5	15.6
				Coefficients			
BChl (LP)	Q_y	−0.2163	0.2901	0.0564	−0.0018	0.0131	0.1549
	Q_x	0.2870	0.4333	−0.7514	0.0164	−0.0725	0.2148
	B_x	−0.0563	−0.0433	0.0145	0.0078	−0.0115	0.0837
	B_y	0.0158	−0.0407	0.0018	0.0032	−0.0076	−0.0429
BChl (MP)	Q_y	0.0599	−0.1498	−0.1660	−0.0006	−0.0155	−0.1898
	Q_x	−0.2858	−0.6032	−0.3664	0.0120	−0.0369	0.5810
	B_x	0.0935	0.0324	−0.0410	−0.0037	0.0053	−0.0061
	B_y	0.0130	0.0384	0.0145	−0.0005	0.0067	0.0576
BChl (LA)	Q_y	−0.0116	0.0055	0.0087	−0.0005	−0.0020	0.0092
	Q_x	0.0200	0.0051	−0.0380	−0.8917	0.4475	0.0417
	B_x	−0.0223	−0.0011	0.0142	0.0017	0.0011	0.0198
	B_y	0.0046	−0.0008	−0.0049	0.0002	0.0011	−0.0085
BChl (MA)	Q_y	0.0223	−0.0158	−0.0122	−0.0016	0.0001	−0.0021
	Q_x	−0.0165	−0.0015	0.0612	−0.4510	−0.8897	−0.0209
	B_x	0.0150	0.0038	−0.0146	0.0010	−0.0007	−0.0156
	B_y	−0.0073	0.0048	0.0073	0.0009	0.0001	0.0019
BPh (L)	Q_y	−0.0079	0.0001	0.0088	0.0119	−0.0067	0.0017
	Q_x	0.0020	0.0018	−0.0105	0.0131	−0.0079	−0.0008
	B_x	0.0020	0.0027	−0.0084	0.0104	−0.0066	0.0003
	B_y	−0.0017	−0.0002	0.0036	0.0050	−0.0027	0.0009

Table I (Continued)

		7	8	9	10	11	12
BPh (M)	Q_y	0.0079	−0.0017	−0.0020	0.0029	0.0081	−0.0027
	Q_x	−0.0036	−0.0009	−0.0027	0.0041	0.0087	0.0115
	B_x	−0.0051	−0.0020	−0.0038	0.0034	0.0081	0.0072
	B_y	0.0017	−0.0002	−0.0005	0.0010	0.0030	−0.0018
CT (L → M)[f]	1	0.4004	0.1894	0.4594	0.0233	−0.0085	0.7048
	2	−0.1076	−0.1933	−0.0240	0.0015	−0.0033	0.1160
	3	−0.0556	−0.0473	−0.0612	−0.0034	0.0015	−0.0749
	4	0.0114	0.0387	−0.0089	0.0001	0.0002	0.0174
CT (M → L)[f]	1	0.7586	−0.4577	−0.0347	0.0001	−0.0075	−0.1516
	2	0.1196	0.1988	−0.2100	0.0027	−0.0187	−0.0222
	3	−0.0782	0.0835	−0.0263	0.0019	−0.0043	0.0273
	4	−0.0018	−0.0490	0.0261	−0.0005	0.0016	−0.0216

[a] Band wavelength (nm). [b] Dipole strength (D^2). [c] Rotational strength ($D \cdot \mu_B$). [d] Linear dichroism (D^2) defined as in the text. [e] Change in permanent dipole moment (D). [f] CT transitions of $BChl_{LP}$ and $BChl_{MP}$.

fundamentally. The wavelengths, dipole strengths, rotational strengths, linear dichroism, and changes in permanent dipole moment associated with the absorption bands are included in the table.

In accord with Figures 1 and 2, the coefficients given in Table I indicate that CT transitions make particularly important contributions to the reaction center's first excited state. The CT transition from ϕ_2 of $BChl_{MP}$ to ϕ_3 of $BChl_{LP}$ has a coefficient comparable to those of the Q_y transitions of the two BChls. The lowest excited state also contains contributions from higher energy CT transitions, from the Q_x, B_x and B_y transitions of $BChl_{MP}$ and $BChl_{LP}$, and from local transitions of the neighboring BChls and BPhs. As noted previously,[9] spreading of the excitation onto $BChl_{LA}$ could play a role in the photochemical transfer of an electron to BPh_L.

Absorption, Linear Dichroism, and CD Spectra. Panels A, B, and C in Figure 3 show complete absorption, linear dichroism, and CD spectra calculated under the assumptions used to generate Table I. The linear dichroism spectrum (Figure 3B) was calculated from the dipole strengths parallel and perpendicular to the reaction center's axis of local C_2 pseudosymmetry. For comparison, panels A, B, and C in Figure 4 show absorption, linear dichroism, and CD spectra obtained experimentally with *Rps. viridis* reaction centers.[9,12,28] The spectral region below 500 nm is not included in Figure 4 because it contains absorption bands of the hemes, carotenoid and protein, which are not considered in the calculations for Figure 3. The absorption band near 555 nm in Figure 4A also is due largely to the hemes. The experimental linear dichroism spectrum (Figure 4B) cannot be compared in detail with the absorption and CD spectra (Figure 4, A and C), because it was measured at a lower temperature (5 K instead of 295 K). The absorption bands sharpen with decreasing temperature, and the long-wavelength band shifts from 960 to approximately 990 nm. We did not attempt to model these effects in the calculated linear dichroism spectrum (Figure 3B); the same wavelengths and bandwidths were used for the bands in this spectrum as for the calculated absorption and CD spectra (Figure 3, A and C). In addition, the calculated linear dichroism is for a perfectly oriented sample, whereas the experimental sample is partially disordered. One can, however, compare the signs of the bands in the calculated and observed linear dichroism spectra, bearing in mind that sharpening or shifting of the bands can alter the spectrum qualitatively in regions where several bands overlap. Note, for example, that the pair of bands at 790 and 798 nm (Table I) are too close together to be resolved in Figure 3B but appear as distinct bands in Figure 4B and that bands with opposite signs tend to cancel in the 830-nm region.

The calculated spectra shown in Figure 3 resemble the experimental spectra remarkably well. In the near-infrared region, similar spectra can be obtained on the assumption that the CT energies for electron transfer in the two directions are identical, as in Figure 1, if one puts the lowest CT energy near 15000 cm^{-1}.

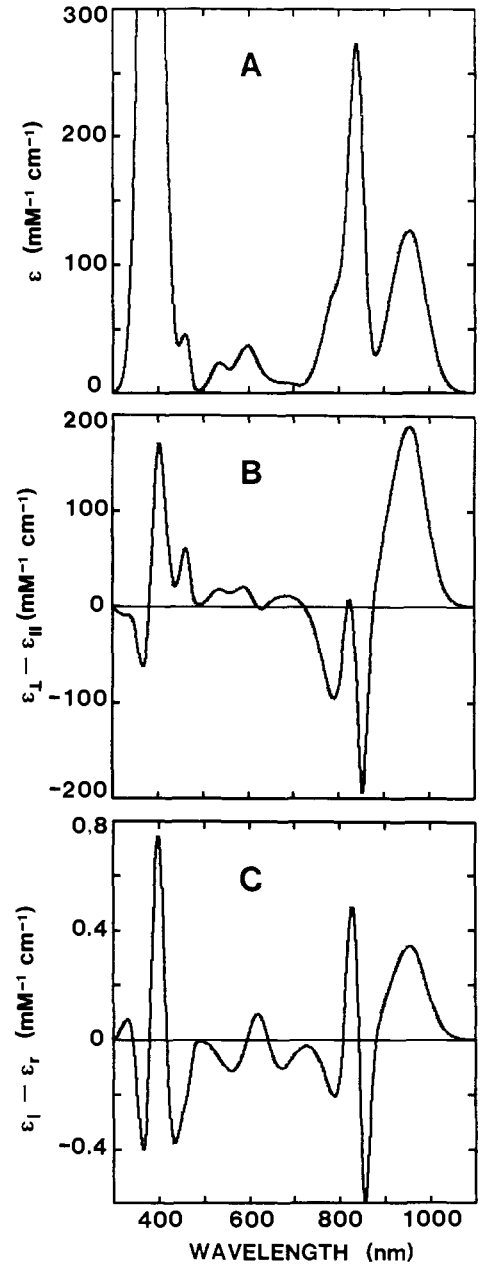

Figure 3. Optical absorption (A), linear dichroism (B), and circular dichroism (C) spectra calculated as Figures 1 and 2 but with the CT transitions from $BChl_{LP}$ to $BChl_{MP}$ 2000 cm^{-1} above the corresponding transitions from $BChl_{MP}$ to $BChl_{LP}$, and with the lowest energy CT transition at 14400 cm^{-1}. In the linear dichroism spectrum, transitions polarized perpendicular to the reaction center's local axis of C_2 pseudosymmetry have positive signs.

(28) Philipson, K. D.; Sauer, K. *Biochemistry* **1973**, *12*, 535–539.

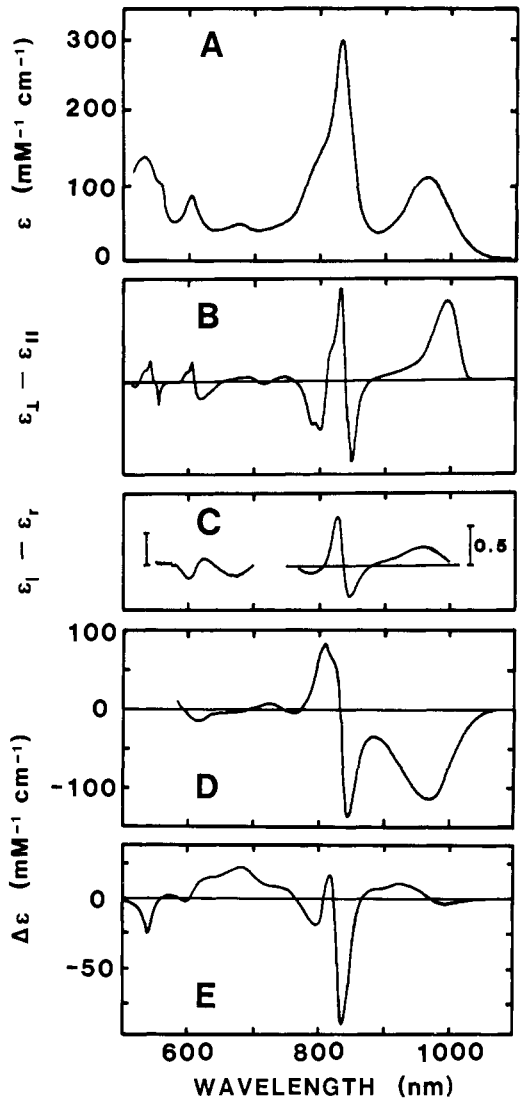

Figure 4. (A) Experimentally measured optical absorption spectrum of *Rps. viridis* reaction centers at 295 K (taken from ref 9). The base line for this spectrum probably rises gradually with decreasing wavelength, due to light scattering. The weak absorption band near 790 nm could be due to a chlorin impurity in the preparation. Much of the absorbance in the 550-nm region and at shorter wavelengths is due to the four bound *c*-type hemes, which are not considered in the calculated spectra (Figure 3). (B) Experimental linear dichroism spectrum of *Rps. viridis* reaction centers at 5 K. The long-wavelength absorption band is at 990 nm at this temperature. The vertical scale in this spectrum is in arbitrary units. (Taken from ref 12.) The linear dichroism is measured with respect to an orientation axis established by compressing a sample in a polyacrylamide gel; this probably is approximately parallel to the reaction center's C_2 axis.[12] (C) Experimental CD spectra of *Rps. viridis* reaction centers at 295 K. The spectrum in the visible region is taken from ref 12 and that in the near-IR is taken from ref 28. The vertical markers represent units of 0.5 mM^{-1} cm^{-1}. (D) Experimental difference spectrum caused by photooxidation of the special pair of BChls in *Rps. viridis* reaction centers at 295 K (taken from ref 36). Under the experimental conditions, the special pair (P) transfers an electron to a quinone (Q), generating the P^+Q^- radical pair. The absorbance changes contributed by Q are not considered in Figure 6, but they are relatively insignificant. (E) Difference spectrum caused by photoreduction of *Rps. viridis* reaction centers by continuous illumination in the presence of $Na_2S_2O_4$ at 295 K (taken from ref 7). Under the experimental conditions BPh_L is converted to a radical anion, while P is held in its resting (unoxidized) state.

In the region between 600 and 700 nm, however, this gives less satisfactory agreement with experiment than is shown in Figure 3. The absorption spectrum then is calculated to include a band at 630 nm with a positive linear dichroism. (This is band 9 in Figure 1A.) The experimental spectra show a band near 620 nm with a *negative* linear dichroism, along with a negative CD band near 670 nm (Figure 4, A, B, and C), and the calculated spectra in Figure 3 account well for these features. Interchanging the assignments of the CT energies, so that electron transfer from $BChl_{LP}$ to $BChl_{MP}$ is more favorable than that from $BChl_{MP}$ to $BChl_{LP}$, leads to poorer agreement with the experimental spectra. The calculated linear dichroism then becomes positive in the 620-nm region, and the CD becomes positive in the 670-nm region (not shown).

The linear dichroism and CD spectra thus support the conclusion that electron transfer from $BChl_{MP}$ to $BChl_{LP}$ is more favorable than electron transfer in the opposite direction. The crystal structure of the *Rps. viridis* reaction center appears to be consistent with this view, because the ketone oxygen on ring V of $BChl_{LP}$ is hydrogen bonded to a threonine residue whereas there is no amino acid in a position to form a similar hydrogen bond with $BChl_{MP}$.[3] The hydrogen bond would stabilize the $BChl^-$ radical of $BChl_{LP}$ relative to the $BChl^+$ radical. The carboxyl ester group on ring V of $BChl_{MP}$ does appear to be hydrogen bonded,[3] but this group is not conjugated to the π-system of the BChl. Electric fields from other parts of the protein also will tend to stabilize the $BChl^-$ radical relative to $BChl^+$ on one side or the other. The hydrogen bonds formed to the acetyl oxygens on ring I of the two BChls also could be important in this regard, but here the differences between $BChl_{LP}$ and $BChl_{MP}$ are less pronounced. (The acetyl oxygen of $BChl_{LP}$ is hydrogen bonded to the side chain of a tryosine residue; that of $BChl_{MP}$, to a histidine.[3]) Functionally, it could be advantageous for electron transfer from $BChl_{MP}$ to $BChl_{LP}$ to be favored, because $BChl_{LP}$ is in a better position to transfer an electron to BPh_L.

Bands 7 and 12 in Table I (681 and 573 nm) represent transitions that are predominantly charge-transfer in character. These make relatively small contributions to the calculated absorption spectrum (Figure 3A) because their dipole strengths are comparatively small. In addition, their bandwidths are expected to be broader than those of the bands that are made up mainly of local transitions, but our choice of 2000 cm^{-1} for the bandwidths is arbitrary (see Methods). The 573-nm band does contribute noticeably to the calculated CD spectrum (Figure 3C), giving a negative CD band at a shorter wavelength than is seen experimentally in this region (Figure 4C). Some possible reasons for this discrepancy will be discussed below.

Energies of the Local Transitions. The energies of the CT transitions have comparatively little effect on the wavelengths of the reaction center's absorption spectrum in the 830-nm region (Figures 1 and 2). The calculated absorption bands at 812, 838, and 849 nm contain contributions from the local transitions of all six pigments, but the contributions from CT transitions are smaller than those in the 960-nm band (Table I). The overall absorption maximum in this region of the calculated spectrum (Figure 3) remains close to the wavelengths chosen for the Q_y transitions of $BChl_{LA}$ and $BChl_{MA}$, because the interactions of these two BChls with each other and with the other pigments are relatively weak. It therefore seems justified to use the experimental spectrum to estimate the effect of the protein on the monomer transition energies. This is done here by setting the wavelength of the Q_y transitions of $BChl_{LA}$ and $BChl_{MA}$ at 830 nm. For simplicity, we assume that, in the absence of the interactions contained in U, all four BChls would have their Q_y bands at this same wavelength. A more detailed analysis of this point should be possible when the X-ray coordinates of the protein are available.

Note that the influence of the CT transitions on the spectra could not be modeled well simply by introducing an additional red shift in the assumed wavelength of the Q_y transitions of $BChl_{LP}$ and $BChl_{MP}$, as Knapp et al.[29,30] have suggested. Such a shift would move both the symmetric and the antisymmetric exciton bands of this pair of molecules to longer wavelengths. For example, if all of the terms involving CT transitions are omitted from

(29) Knapp, E. W.; Fischer, S. F. In *Antennas and Reaction Centers of Photosynthetic bacteria*; Michel-Beyerle, M. E., Ed.; Springer-Verlag: Berlin, 1985; pp 103–108.

(30) Knapp, E. W.; Fischer, S. F.; Zinth, W.; Sander, M.; Kaiser, W.; Deisenhofer, J.; Michel, H. *Proc. Natl. Acad. Sci. U.S.A.* **1985**, *82*, 8463–8467.

the interaction matrix, the long-wavelength absorption band can be made to occur at 960 nm by moving the Q_y transitions of $BChl_{LP}$ and $BChl_{MP}$ to 930 nm, but the second absorption band then occurs at 915 nm instead of 849 nm. (Knapp et al.[29,30] compensate for this effect by using a larger value for the Q_y exciton interaction matrix element.) In our analysis, decreasing the energy of the CT transitions has a pronounced effect on the long-wavelength absorption band, while the bands in the region between 790 and 850 nm hardly move (Figure 2A). The dipole strengths and rotational strengths of the bands in the 830- and 850-nm regions do rearrange (Figure 2, B and C), but not in the same manner that they do if the transition energies for $BChl_{LP}$ and $BChl_{MP}$ are simply shifted to longer wavelengths.

To bring the calculated linear dichroism spectra into accord with the experimental, we assigned different energies for the local transitions of the two bacteriopheophytins. BPh_L was assumed to have its Q_y and Q_x transitions at 805 and 545 nm; the Q_y and Q_x transitions of BPh_M were put at 795 and 535 nm. The choice of 545 nm for the Q_x transition of BPh_L is in accord with the observation that photoreduction of BPh_L causes a bleaching here, while little bleaching occurs in a companion band at 535 nm.[7,31-34] The choices for the Q_y transitions make the calculated absorption band at 790 nm (band 6 in Figure 2 and Table I) polarized perpendicular to the reaction center's crystallographic z-axis, whereas the band at 798 nm (band 5) is polarized parallel to this axis. (For band 5, the dipole strength calculated parallel to the z-axis is 19.3 D^2, and that perpendicular to the z-axis is 1.6 D^2. For band 6, the parallel component is 0.3 D^2; the perpendicular, 27.8. These features are not shown in Figure 3B, which pertains to a different polarization axis.) This agrees with the dichroism seen experimentally with oriented crystals of *Rps. viridis* reaction centers.[30] Reversing the assignments of the Q_y transitions of BPh_L and BPh_M gives the opposite polarization. The difference between the transition energies of the two bacteriopheophytins can be attributed plausibly to the fact that the ketone oxygen of BPh_L is hydrogen bonded to a glutatmic acid residue, whereas the oxygen of BPh_M is free.[3]

Other Indications of the Importance of CT Transitions: The Stark Effect and the Width of the Long-Wavelength Band. A major contribution of CT transitions to the long-wavelength absorption band is consistent with the observation that external electric fields cause an unusually large Stark effect on this band in reaction centers of both *Rhodobacter sphaeroides*[35,36] and *Rps. viridis* (S. Boxer, personal communication). As shown in Table I, the change in permanent dipole moment associated with the 960-nm band in *Rps. viridis* is calculated to be approximately 3 D and is larger than those associated with the other bands in the near-infrared region. The vector describing the change in dipole moment makes an angle of approximately 32° with respect to the 960-nm optical transition dipole. The effects of an external electric field on the reaction center's absorption spectrum cannot be calculated simply from the changes in dipole moments associated with the absorption bands; one needs to rediagonalize **U** after introducing the perturbations due to the field. However, the dipole moments do indicate that the long-wavelength band will be particularly sensitive to external fields. (A more detailed analysis of this point will be presesented elsewhere; see also ref 36 and 37.) In Table I and Figure 3, the CT transitions from $BChl_{LP}$ to $BChl_{MP}$ are assumed to lie 2000 cm^{-1} above the corresponding transitions from $BChl_{MP}$ to $BChl_{LP}$. If the separation is increased to 4000 cm^{-1}, as in Figure 2, the calculated change in dipole moment for the 960-nm band increases to 4.8 D. In contrast, if the CT transitions in opposite directions are made degenerate, as in Figure 1, the change in dipole moment associated with the long-wavelength band is calculated to be only 0.1 D. This is because the first excited state then contains nearly equal contributions from CT transitions in opposite directions. The Stark effect therefore supports the views that CT transitions make important contributions to the absorption spectrum and the CT transitions of the special pair are asymmetrical.

Charge-transfer transitions may also provide a basis for rationalizing the broad width of the long-wavelength absorption band, as measured in recent laser hole-burning and photon-echo experiments, because one would expect such transitions to be strongly coupled to nuclear motions.[2-24,38] The sensitivity of the CT energies and the interaction matrix elements to the geometry of the BChl complex and to solvation of the BChl radicals by the protein has been discussed above and in the previous paper.[8] The potential surfaces that have been calculated for the ground and excited states of a chlorophyll *a* dimer[26] suggest that nuclear relaxation of the lowest excited electronic state could make a major contribution to the observed bandwidth. A significant broadening of the band also could be associated with relaxation of the protein. However, our results do not support the suggestion[20,21] that the large bandwidth reflects a relaxation of the excited reaction center from an excitonic $\pi-\pi^*$ state to a pure CT state. The conclusion that we have drawn from Figures 1 and 2 is that the lowest CT state lies *above* the exciton state. As shown in Figure 3A of the accompanying paper,[8] the energy of the CT state approaches that of the exciton state upon reduction of the intermolecular distance between $BChl_{LP}$ and $BChl_{MP}$, but the two states do not cross.

Sensitivity of the Spectrum to Nuclear Geometry. As was illustrated in the previous paper,[8] the interactions between local molecular transitions and CT transitions in a BChl dimer depend strongly on the geometry of the complex. Figure 5A shows the calculated wavelength of the first six absorption bands of the reaction center as a function of the distance between the planes of $BChl_{LP}$ and $BChl_{MP}$. For these calculations, $BChl_{1P}$ was kept fixed in position relative to $BChl_{LA}$, BCl_{MA}, and the two BPhs, and $BChl_{MP}$ was translated along the axis determined by the cross product of its N1 → N3 vector and the corresponding vector of $BChl_{LP}$ (see Figure 1B of ref 8). As the distance between the two molecules decreases below 3.6 Å, the long-wavelength absorption band moves sharply toward the near-IR. In the region around 3.1 Å (the distance found in the *Rps. viridis* reaction center), a displacement of 0.1 Å shifts the absorption maximum by about 25 nm. This slope depends somewhat on our assumption of an effective dielectric constant of 3.0 in calculating how the energies of the CT transitions vary with the geometry of the complex (see Methods). If a dielectric constant of 1.0 is used, a displacement of 0.1 Å shifts the absorption maximum by about 27 nm. A dielectric constant on the order of 3 is expected for excited states, as long as the permament dipoles of the protein are polarized by the ground-state charge distribution in the chromophores; induced dipoles of the protein contribute a dielectric constant of about 2 for charge–charge interactions.[17] It should be possible to evaluate the actual effective dielectric constant when the X-ray structure of the protein is known. As noted above, the dielectric constant is expected to depend on the time available for relaxation of the protein around the dimer.[17]

In contrast to the long-wavelength band, the absorption bands between 790 and 850 nm are relatively insensitive to the distance between the planes of $BChl_{LP}$ and $BChl_{MP}$ (Figure 5A). This differs from the result that is obtained by considering just the special pair of BCls alone, without including interactions with the neighboring molecules. In that case, the energy of the second absorption band also moves to longer wavelengths as the distance between the molecules is decreased, although it is still less sensitive to the distance than the long-wavelength band is (see curve 4a in Figure 3A of ref 8). The increased stability of the bands in

(31) Shuvalov, V. A.; Krakhmaleva, I. N.; Klimov, V. V. *Biochim. Biophys. Acta* **1976**, *449*, 597–601.
(32) Netzel, T. L.; Rentzepis, P. M.; Tiede, D. M.; Prince, R. C.; Dutton, P. L. *Biochim. Biophys. Acta* **1977**, *460*, 467–479.
(33) Thornber, J. P.; Cogdell, R. J.; Seftor, R. E. B.; Webster, G. D. *Biochim. Biophys. Acta* **1980**, *593*, 60–75.
(34) Kirmaier, C.; Holten, D.; Parson, W. W. *Biochim. Biophys. Acta* **1985**, *810*, 49–61.
(35) deLeeuv, D.; Malley, M.; Butterman, G.; Okamura, M.; Feher, G. *Biophys. J.* **1982**, *27*, 111a.
(36) Lockhart, D. J.; Boxer, S. G. *Biochemistry* **1987**, *26*, 664–668.
(37) Scherer, P. O. J.; Fischer, S. F. *Chem. Phys. Lett.* **1986**, *131*, 153–159.
(38) Friesner, R. *Proc. Natl. Acad. Sci. U.S.A.*, in press.

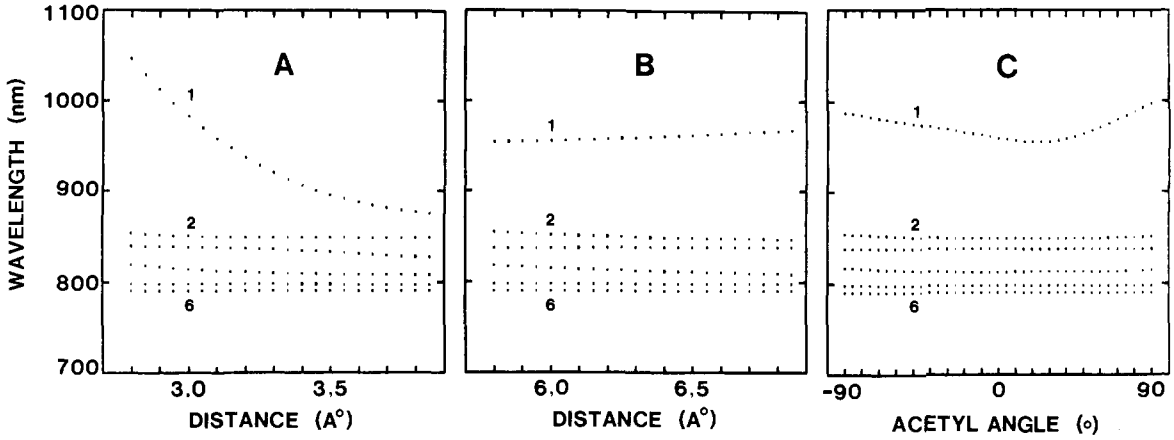

Figure 5. Calculated wavelengths of the *Rps. viridis* reaction center's first 6 absorption bands, as functions of the position of $BChl_{MP}$ (A, B) and of the orientation of the acetyl group of $BChl_{LP}$ (C). For the reaction center's initial geometry, the energies asigned to the CT transitions were as in Figure 3. As the geometry was varied, the energies were corrected according to eq 5a, 6, and 21 of ref 8, with the Coulomb integral ($\gamma_{s,t}$) reduced by an effective dielectric constant of 3. In part A, $BChl_{LP}$ is translated along the axis determined by the cross product of the N1 → N3 vectors of $BChl_{LP}$ and $BChl_{MP}$ (see Figure 1B of ref 8). The abscissa gives the distance between the molecular centers of $BChl_{LP}$ and $BChl_{MP}$ as projected on the translation axis and is a measure of the distance between the planes of the two BChls. In the initial geometry, this distance is approximately 3.1 Å. In part B, $BChl_{LP}$ is translated along the axis defined by subtracting the N1 → N3 vector of $BChl_{LP}$ from the N1 → N3 vector of $BChl_{MP}$. This motion keeps the distance between the molecular planes constant but changes the extent to which the BChls overlap each other in ring I. The abscissa is the projection of the center-to-center distance on the translational axis, which is approximately 6.3 Å in the initial structure. In part C, the abscissa is the torsional angle ($\varphi_{C3,C20}$) of the C3–C20 bond of $BChl_{LP}$ with respect to the plane defined by C4, C3, and C20 (see Figure 1A of ref 8). The angle is defined to be zero in the initial structure, in which oxygen atom O1 is approximately in the plane.[3] The distance between oxygen atom O1 of $BChl_{LP}$ and the Mg atom of $BChl_{MP}$ is minimal (approximately 2.0 Å) when $\varphi_{C3,C20} \approx 75°$.

the reaction center reflects the fact that, when the interactions of the special pair with its neighbors are considered, the second absorption band acquires a major contribution from the Q_y transition of $BChl_{LA}$, along with somewhat smaller contributions from the transitions of $BChl_{MA}$ and BPh_L (Table I). It thus is no longer accurate to consider the 849-nm band as being primarily a symmetric exciton band of $BChl_{LP}$ and $BChl_{MP}$ (see, e.g., ref 12 and 33). Although the Q_y transitions of $BChl_{MP}$ and $BChl_{LP}$ do make a major contribution to this band, the contribution from $BChl_{LP}$ is calculated to be smaller than that from $BChl_{LA}$, and about the same as those from $BChl_{MA}$ and BPh_L (Table I).

Figure 5B shows the results of calculations in which $BChl_{MP}$ was translated along the axis defined by subtracting the N1 → N3 vector of $BChl_{LP}$ from the N1 → N3 vector of $BChl_{LP}$. Since the two vectors are approximately antiparallel, the translation axis in this case is approximately parallel to the N1 → N3 vector of $BChl_{LP}$. Movements along this axis have little effect on the energies of any of the first six absorption bands.

Another geometrical parameter that could play an important role in determining the wavelength of the first absorption band is the orientation of the acetyl group on ring I of each of the BChls in the special pair. Figure 5C shows the calculated wavelength of the absorption bands in the near-IR region as functions of the orientation of the acetyl group on $BChl_{LP}$. In the *Rps. viridis* reaction center, the acetyl group is oriented approximately in the plane of the BChl, so that the torsional angle that forms the abscissa in the figure is close to 0°.[3] If the acetyl group is rotated by ±90°, the position of the lowest energy absorption band varies over a range of about 50 nm. Again, the motion hardly affects the other absorption bands in the near-IR region. Rotating the acetyl group on $BChl_{MP}$ has similar effects (not shown).

The shift of the lowest energy absorption band to longer wavelengths as the acetyl group on $BChl_{LP}$ or $BChl_{MP}$ is rotated results largely from a decrease in the Q_y transition energy of the individual BChl. A rotation of ±90° lowers the transition energy by about 360 cm^{-1}. As noted in Methods, our calculations on this point are approximate because we did not redetermine the molecular orbital coefficients and CI coefficients for each value of the torsional angle. Assumptions concerning the dielectric constant do not affect the results significantly in this case.

One spectroscopic property of reaction centers that has been particularly puzzling is that the long-wavelength absorption band shifts to even longer wavelengths with decreasing temperature, while the bands in the 830-nm region (or the corresponding bands in the 800-nm region in reaction centers that contain BChl-*a*) sharpen but do not move. The long-wavelength band of *Rps. viridis* reaction centers moves from 960 nm at 295 K to 990 nm at 5 K.[12] The calculations shown in Figure 5 suggest that this shift could reflect a rotation of one or both of the acetyl groups on $BChl_{LP}$ and $BChl_{MP}$ or a decrease in the intermolecular distance between the two BChls. In the *Rps. viridis* reaction center, the acetyl oxygens are hydrogen bonded to tyrosine and histidine side chains[3] and might be pulled out of plane by movements of the protein.

Absorption Changes Caused by Electron Transfer. By omitting the transitions that involve $BChl_{LP}$ and $BChl_{MP}$ from the calculations, one can model the spectroscopic properties of reaction centers in which the special pair of BChls has been photooxidzed or converted to an excited triplet state. The dotted curve in Figure 6A shows the *changes* that omitting these BChls cause in the calculated absorption spectrum. For comparison, Figure 4D shows the experimentally measured difference between the absorption spectra of photooxidzed and resting reaction centers.[39] The main feature in such a difference spectrum is the disappearance of the long-wavelength absorption band. The blue shift of the absorption band in the 830-nm region, which is reflected by an absorbance increase on the short-wavelength side of this band and a decrease at longer wavelengths, can be accounted for partly by the loss of the interactions of the special pair of BChls with $BChl_{LA}$ and $BChl_{MA}$ and by the disappearance of the higher energy exciton transitions of the special pair. As was noted above (Table I) the 798-, 812-, 838-, and 849-nm absorption bands of the resting reaction centers contain extensively mixed contributions from all four BChls. In addition, the electric field from the cationic $BChl^+$ radical (P^+) is expected to cause a shift of the absorption bands of $BChl_{LA}$ and $BChl_{MA}$. The solid curve in Figure 6 includes this electrochromic effect, which is calculated to be relatively small. The absorption spectrum of P^+ is neglected in the calculations, although it may contribute to the absorbance increase on the short-wavelength side of the 830-nm band.[40]

The absorption changes caused by photoreduction of BPh_L can be modelled by omitting the transitions that involve this molecule and including the electrochromic effects of BPh_L^-. The dotted

(39) Prince, R. C; Tiede, D. M.; Thornber, J. P.; Dutton, P. L. *Biochim. Biophys. Acta* **1977**, *462*, 467–490.
(40) Vermeglio, A.; Breton, J.; Paillotin, G.; Cogdell, R. J. *Biochim. Biophys. Acta* **1978**, *501*, 514–530.

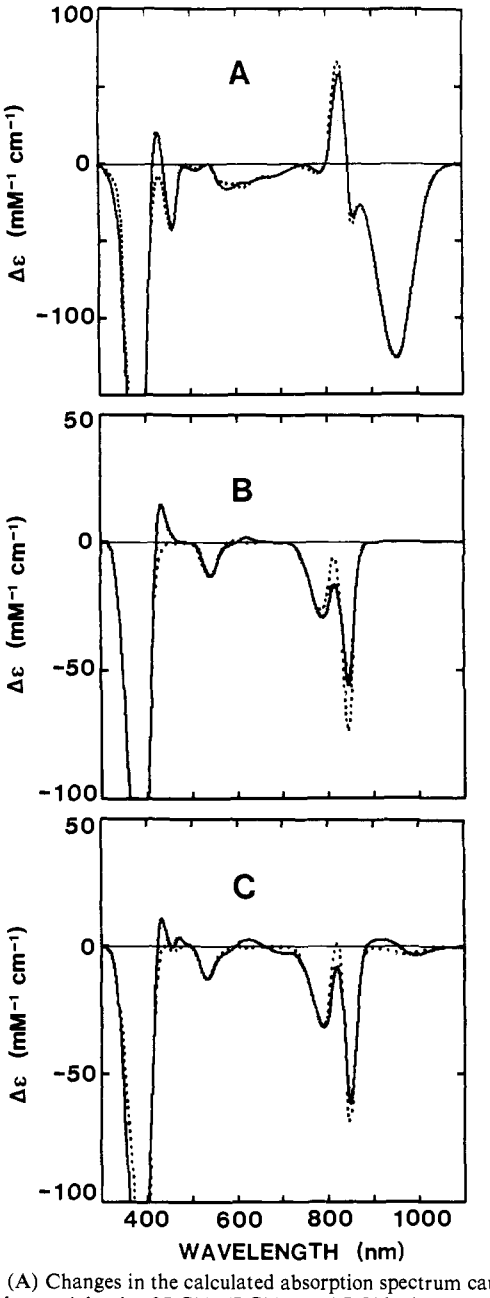

Figure 6. (A) Changes in the calculated absorption spectrum caused by omitting the special pair of BChls ($BChl_{LP}$ and $BChl_{MP}$). Assumptions as in Figure 3. This calculation models some of the absorption changes that are observed upon photooxidation of the special pair (P) to the radical cation, P^+ (Figure 4D). The difference spectrum graphed with a solid line includes the electrochromic effects of P^+ on the other pigments; that graphed with a dotted line neglects these effects. The absorption bands of P^+ itself are not considered. (B) Changes in the calculated absorption spectrum caused by omitting BPh_L. These model the observed absorption changes associated with the reduction of BPh_L when P is held in its resting, unoxidized state (Figure 4E). The solid curve includes electrochromic effects of BPh_L^- on the other pigments; the dotted curve neglects these effects. The calculations do not consider the absorption bands of the reduced BPh. (C) Changes in the calculated spectrum caused by omitting BPh_L when the special pair of BChls has already been omitted. These model the absorption changes associated with the transient reduction of BPh_L when P is in the oxidized state, P^+ (not shown in Figure 4). Electrochromic effects of both P^+ and BPh_L^- are included in the solid curve and are neglected in the dotted curve.

curve in Figure 6B shows the changes that simply omitting BPh_L causes in the calculated absorption spectrum. Electrochromic effects of BPh_L^- on the other molecules are included in the spectrum shown as a solid curve. Figure 4E shows an experimentally measured difference spectrum obtained by illuminating *Rps. viridis* reaction centers continuously in the presence of a strong reductant.[7] In addition to absorbance decreases at 545 and 800 nm, which one expects to see upon reduction of BPh_L, the experimental difference spectrum includes a partial bleaching and blue shift of the absorption band in the 830-nm region. It has been controversial whether the bleaching results simply from the reduction of BPh_L or instead reflects reduction of $BChl_{LA}$.[7,31-34,41-45] In the calculations (Figure 6B), a bleaching in the 830-nm region occurs simply upon removal of BPh_L. This reflects the fact that the absorption bands at 812, 838, and 849 nm contain significant contributiuons from the BPh, in addition to contributions from the four BChls (Table I). Because of the mixed nature of the absorption bands, the magnitude of the bleaching at 830 nm can exceed that seen at 800 nm. Other features that can be seen in both the calculated and experimental spectra are a blue shift of the 960-nm absorption band and a red shift of the 600-nm band. The absorbance increase seen experimentally in the 650-nm region (Figure 4E) can be attributed to the BPh_L^- radical,[46] which is not included in the calculations.

Figure 6C shows the changes in the calculated absorption spectrum resulting from leaving out BPh_L when the special pair of BChls has already been omitted. This models the difference spectrum obtained in picosecond kinetic experiments,[7,34,43-45] in which the flash-induced absorption changes measured at 1–2 ns after the excitation flash are subtracted from the absorption changes measured at 20–40 ps after the flash. The special pair of BChls is in the oxidzed state at both times; BPh_L is in the reduced state at the earlier time but has transferred an electron to a quinone by the later time. Again, the calculated difference spectrum shows a bleaching in the 830-nm region. Because oxidizing the special pair of BChls alters the composition of all of the absorption bands, it is not surprising that the relative magnitudes of the absorbance changes at 800 and 830 nm are different in Figure 6C than they are in Figure 6B. The sensitivity of the excited states to nuclear geometry could provide an explanation for the complicated wavelength dependence that has been described for the decay kinetics of the absorbance changes in this region of the spectrum.[34] If reaction centers occur with a distribution of different geometries, a higher rate of electron transfer in one subgroup of the population could be correlated indirectly with a larger absorbance change at 830 nm relative to 800 nm.

Charge-Transfer Transitions Involving $BChl_{LA}$ and $BChl_{MA}$. At cryogenic temperatures, the long-wavelength absorption band of *Rps. viridis* reaction centers reveals a shoulder near 1020 nm. The shoulder has been suggested to be a CT band reflecting the transfer of an electron from P to one of the neighboring BChls.[47-49] To explore this interpretation, we expanded the interaction matrix **U** to include the 16 additional CT transitions in which an electron is transferred from either $BChl_{LP}$ or $BChl_{MP}$ to $BChl_{LA}$ or $BChl_{MA}$. The 16 CT transitions for electron transfer from $BChl_{LA}$ or $BChl_{MA}$ to the special pair also were included, increasing **U** to a 64 × 64 matrix. Because of the larger intermolecular distances, the orbital overlap of $BChl_{LP}$ and $BChl_{MP}$ with the neighboring BChls is much weaker than that between the two molecules of the special pair. The matrix elements describing the interactions of the Q_y transition of $BChl_{LP}$ with the CT transitions in which an electron moves from ϕ_2 of this BChl to ϕ_3 of $BChl_{LA}$ or $BChl_{MA}$ are only −6.7 and −1.4 cm^{-1}, respectively, compared to the matrix element of about 870 cm^{-1} for the interaction of this Q_y transition

(41) Shuvalov, V. A.; Asadov, A. A. *Biochim. Biophys. Acta* **1979**, *545*, 296–308.
(42) Parson, W. W. *Annu. Rev. Biophys. Bioeng.* **1982**, *11*, 57–80.
(43) Kirmaier, C.; Holten, D.; Parson, W. W. *Biochim. Biophys. Acta* **1983**, *725*, 190–192.
(44) Kirmaier, C.; Holten, D.; Parson, W. W. *FEBS Lett.* **1985**, *185*, 76–82.
(45) Shuvalov, V. A.; Amesz, J.; Duysens, L. N. M. *Biochim. Biophys. Acta* **1986**, *851*, 327–330.
(46) Fajer, J.; Davis, M. S.; Brune, D. C.; Forman, A.; Thornber, J. P. *J. Am. Chem. Soc.* **1978**, *100*, 1918–1920.
(47) Vermeglio, A.; Paillotin, G. *Biochim. Biophys. Acta* **1982**, *681*, 32–40.
(48) Shuvalov, V. A.; Klevanik, A. V. *FEBS Lett.* **1983**, *160*, 51–55.
(49) Maslov, V. G.; Klevanik, A. V.; Ismailov, M. A.; Shuvalov, V. A. *Dokl. Akad. Nauk SSSR* **1983**, *269*, 1217–1221.

with the movement of an electron to $BChl_{MP}$. The matrix elements for the interactions of the Q_y transition of $BChl_{MP}$ with the CT transitions from ϕ_2 of this BChl to ϕ_3 of $BChl_{LA}$ or $BChl_{MA}$ are 0.2 and −2.9 cm^{-1}. CT transitions involving $BChl_{LA}$ and $BChl_{MA}$ thus are calculated to make only very small contributions to the absorption spectrum. An absorption shoulder can be obtained in the 1000-nm region if one assumes that the CT transition for electron transfer from ϕ_2 of $BChl_{MP}$ to ϕ_3 of $BChl_{LA}$ has an energy of approximately 10900 cm^{-1}, but the dipole strength calculated for the shoulder is only about 0.03 D^2. This is much smaller than the dipole strength of approximately 115 D^2 calculated for the main long-wavelength band.

It thus seems likely that the long-wavelength shoulder in the experimental absorption spectrum reflects structural heterogeneity of the reaction centers,[50] rather than a CT absorption band. Charge-transfer transitions involving $BChl_{LA}$ are, however, likely to play an important role in the transfer of an electron from P to BPh_L. Calculations aimed at exploring this point are in progress.[51]

Concluding Remarks

Molecular Models vs. Phenomenological Models. The philosophy of this work and related studies[25,26] is basically orthogonal to the more conventional phenomenological approach (e.g., ref 10, 29 and 30). In this section, we discuss some of the differences and point out benefits of the more complicated approach of using explicit molecular models.

In the phenomenological approach, one tries to extract effective parameters by *fitting* a simple (and sometimes oversimplified) model to the available experimental information. This can be quite instructive, as long as one is not concerned with the actual details of a highly complex system. But the reaction center, like many biological molecules, is so complicated that its detailed behavior cannot be predicted reliably by a model that has only a few parameters. In such systems there often is no unique way of extracting the actual molecular parameters from the experimental information. This is apparent, for example, in phenomenological attempts to evaluate the distribution of the reorganization energy in electron-transfer processes (see discussion in ref 26).

The approach we have followed here is to attempt to *calculate* the properties of the reaction center, using explicit models for all of the system's individual components. These models are indeed parameterized, but only for properties of the isolated components and related molecules, and not for the properties of the actual system under study. Comparisons of the calculated and observed properties are used as a *check* rather than as a calibration of the explicit model; obtaining reasonable agreement with the experimental results indicates that other properties that are not observed directly can be estimated in a reasonable way. For example, if the reaction center's spectroscopic properties are reproduced without significant adjustment, then the CT matrix elements (which are not observed directly but play a crucial role in the electron-transfer process) probably have been estimated reasonably.

In evaluating the interaction matrix elements, we found both exciton interactions and CT interactions to be important. Previous phenomenological studies that fit the observed spectra to a simple exciton model[29,30] had to use larger exciton coupling terms than those obtained in the direct calculations, since the CT interactions were not considered. To account for the red shift of the long-wavelength absorption band, it also was necessary to assume that the local Q_y transition energies of $BChl_{LP}$ and $BChl_{MP}$ were substantially lower than those of $BChl_{LA}$ and $BChl_{MA}$. (We assumed that these energies were all the same.) The phenomenological apprach did provide a satisfactory fit of the absorption spectrum, but when additional experimental information on the Stark effect was considered it became clear that the model needed to be modified to include CT transitions.[37]

Although phenomenological stuidies are often described as calculations, the term "calculation" then takes on a rather different meaning. For example, estimating the effective dipole moment of the excited state from the observed Stark effect[37] is not a "calculation" in our sense but rather a phenomenological fitting that can be done only when the corresponding experimental information is available. Calculating the excited state dipole moment from a molecular model that has no built-in information about the Stark effect is fundamentally different in that it represents an unbiased prediction of the observation.

Comparisons with Experiment. The theory discussed here appears to account well for the absorption and linear dichroism spectra of *Rps. viridis* reaction centers and for the absorption changes that occur when the special pair of BChls transfers an electron to BPh_L or to a quinone. The rotational strengths of the major bands in the CD spectrum also are predicted reasonably accurately, although that of the 838-nm band appears to be underestimated somewhat relative to the strengths of the other bands, and the negative band in the 570-nm region is located at shorter wavelengths than the band seen in this region experimentally. We were not able to improve the calculated CD spectrum significantly by making small changes in the excitation energies assigned to the pigments or the CT transitions. Some of the discrepancies in the CD spectrum could be due simply to the bandwidths that we used for illustrating the spectra. As was noted above, the negative CD band in the 570-nm region is particularly sensitive to the choice of the bandwidth and we have no independent information on which to base this choice. The discrepancies also could be due to our neglect of the vibrational structure of the absorption bands. The Q_y and Q_x absorption bands of monomeric BChl and BPh have pronounced vibronic shoulders on their short-wavelength sides,[10,11] and our treatment simply includes these shoulders in the main absorption bands. Phenomenological approaches that may provide a useful treatment of the vibronic structure of exciton bands have been developed recently.[38,52-54] Another possible source of error is our use of simple first-order perturbation theory to find G, the contributions of doubly excited states to the ground state.[8,10] The calculated CD spectrum is altered markedly if these contributions are neglected, but we have not explored this point in detail. In addition, we have not considered exciton interactions of the pigments with aromatic amino acids, which appear to contribute significantly to the CD spectra of hemoglobin and myoglobin.[55] In the *Rps. viridis* reaction center there are numerous phenylalanine, tyrosine, and tryptophan residues in close contact with the pigments.[3]

Our treatment depends in part on the excitation energies of the local Q_y, Q_x, B_x, and B_y transitions of the six pigments, as well as on the energies of the CT transitions between $BChl_{LP}$ and $BChl_{MP}$. For simplicity, we have assumed that the transition energies of all four BChls are the same. We also have used the same set of molecular orbital coefficients for all four BChls. Because of the differences in the local environments of the pigments, these assumptions cannot be strictly correct. More refined calculations that take into account the different hydrogen-bonding structures of the BChls are in progress. For completion, these calculations require the X-ray coordinates of the protein, which are not yet available.

One of our principal conclusions is that the energy of the lowest CT transition is on the order of 14000 cm^{-1}, which is significantly greater than the energy of the local Q_y transitions of the BChls. This implies that the reaction center probably does not relax from a π-π^* state to a pure CT state of the special pair prior to electron transfer to the BPh. However, the CT transitions of the special pair of BChls evidently do make a major contribution to the reaction center's lowest excited state. The CT transitions appear to be asymmetric, so that electron transfer from $BChl_{MP}$ to $BChl_{LP}$

(50) Hoff, A.; Lous, E. J.; Moehl, K. W.; Dijkman, J. A. *Chem. Phys. Lett.* **1985**, *114*, 39-43.
(51) Parson, W. W.; Creighton, S.; Warshel, A. In *Primary Reactions of Photobiology*; Kobayashi, T., Ed.; Springer-Verlag: Berlin, in press.
(52) Friesner, R.; Silbey, R. *Chem. Phys. Lett.* **1981**, *84*, 365-369.
(53) Friesner, R. *J. Chem. Phys.* **1982**, *76*, 2129-2135.
(54) Dewey, T. G. *J. Chem. Phys.* **1985**, *83*, 486-491.
(55) Hsu, M.-C.; Woody, R. W. *J. Am. Chem. Soc.* **1971**, *93*, 3515-3525.

is more favorable than electron transfer in the opposite direction. This conclusion rests on a comparison of the experimentally observed spectra with the calculated spectra that are obtained under various assumptions concerning the CT energies. It also is in harmony with the sensitivity of the long-wavelength absorption band to external electric fields.

The formalism that we have developed here can be extended straightforwardly to explore the mechanism of the photochemical electron-transfer reaction. Preliminary results, reported in ref 51 and 56, give a coupling matrix element of 5.9 cm^{-1} for the formation of $P^+BChl_{LA}^-$ from the excited reaction center (P*), and 15 cm^{-1} for the subsequent hopping of an electron to BPh_L. An alternative intermediate CT state, $BChl_{LA}^+BPh_L^-$, can be generated from P* with a matrix element of 2.5 cm^{-1} and then relax to $P^+BPh_L^-$ with a matrix element of 11 cm^{-1}.

Acknowledgment. This work was supported by National Science Foundation Grants PCM-8303385, PCM-8312371, and PCM-8316161. We also acknowledge with thanks the help of the ISIS program from Digital Equipment Corp. in obtaining the MicroVax II computer on which the calculations were done. We thank J. Deisenhofer and H. Michel for providing the crystallographic coordinates and J. Breton, D. Holten C. Kirmaier, M. Gouterman, D. Middendorf, R. Pearlstein, and A. Scherz for helpful discussion.

(56) Warshel, A.; Creighton, S.; Parson, W. W., submitted for publication.

A Rhodopsin Pigment Containing a Spin-Labeled Retinal

Geoffrey E. Renk, Yat Sun Or, and Rosalie K. Crouch*

Department of Ophthalmology, Medical University of South Carolina, Charleston, South Carolina 29425. *Received January 2, 1987*

Abstract: A retinal derivative containing a nitroxide group has been synthesized and a photosensitive pigment formed between the 9-cis isomer and bovine opsin. The pigment is stable to hydroxylamine and 11-*cis*-retinal. The electron spin resonance spectrum of the pigment in suspension shows that the nitroxide is strongly immobilized ($\tau > 10^{-7}$ s), is inaccessible to small hydrophilic reagents, and is not highly oriented within the membrane. The electron spin resonance spectrum of detergent-solubilized pigment is highly sensitive to the nature of the detergent, the digitonin and CHAPS solubilized pigment showing spectra most closely resembling the spectrum of pigment in suspension. These data are consistent with the ring portion of the retinal chromophore being deep within the membrane in a hydrophobic environment.

The use of synthetic analogues of retinal to probe the binding site and photochemistry of both the visual pigment rhodopsin and bacteriorhodopsin from the purple membrane of *Halobacterium halobium* has been well established. This approach has been used to ascertain the minimal structural requirements for pigment formation[1,2] and has contributed significantly to understanding of the primary photochemical event in vision.[3] Analogues incorporating the nitroxide "reporter" group are especially well suited to study the protein environment of the chromophore and the motional behavior of these membrane proteins through the use of electron spin resonance (ESR) spectroscopy.[4] We have used this approach to study the binding site of the purple membrane with a spin-labeled derivative of retinal (**1**) in which the nitroxide-containing ring was joined to the retinal ring by an ester linkage[5] and with a second derivative **2** incorporating the nitroxide into the retinal itself, which more closely resembled the parent molecule.[6] The ester **1** was limited in application by protein-mediated hydrolysis which liberated the nitroxide from the membrane. The second nitroxide derivative **2** formed a stable bacteriorhodopsin pigment but failed to combine with bovine opsin to form a pigment (unpublished results).

We report here the synthesis of a new spin-labeled retinal (SLR) **3** that differs from the previous analogue **2** only in that the nitroxide-containing ring lacks a carbon–carbon double bond. This

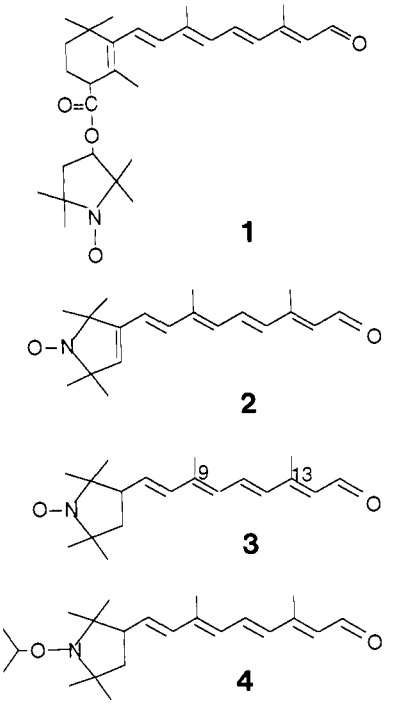

modification in the structure of the SLR now allows the 9-cis isomer to form a stable pigment when combined with bovine opsin, representing the first report of an opsin pigment containing a spin-labeled retinal. This product fulfills the standard criteria for stable photosensitive rhodospin analogue pigments, and the ESR spectrum is consistent with the photochemical behavior. The retinal binding site is shown to be hydrophobic in nature and excludes water from the ring end of the chromophore. The temperature dependence of the ESR spectrum and the effects of detergent solubilization on the ESR data are described.

(1) Balogh-Nair, V.; Nakanishi, K. In *New* Comprehensive *Biochemistry*; Tamm, C., Ed.; Elsevier Biomedical: Amsterdam, 1982; Vol. 3, pp 283–334.
(2) Crouch; R.; Or, Y. S. *FEBS Lett.* **1983**, *158*, 139–142.
(3) Buchert, J.; Stefancic, V.; Doukas, A. G.; Alfano, R. R.; Callender, R. H.; Pande, J.; Akita, H.; Balogh-Nair, V.; Nakanishi, K. *Biophys. J.* **1983**, *43*, 279–283.
(4) Seally, R.; Hyde, J. S.; Antholine, W. In *Modern Physical Methods in Biochemistry*; Neuberger, A., Van Deenen, L. L., Eds.; Elsevier: Amsterdam, 1986; pp 84–120.
(5) Renk, G.; Grover, T.; Crouch, R.; Mao, B.; Ebrey, T. G. *Photochem. Photobiol.* **1981**, *33*, 489–494.
(6) Crouch, R. K.; Ebrey, T. G.; Govindjee, R. *J. Am. Chem. Soc.* **1981**, *103*, 7364–7366.
(7) Hideg, K.; Hankovszky, H. O.; Lex, L.; Kulcsar, G. Y. *Synthesis* **1980**, *11*, 911–914.

0002-7863/87/1509-6163$01.50/0